J. Fluid Mech. (1982), *vol.* 119, *pp.* 297–321
Printed in Great Britain

An experimental study of pressure fluctuations on fixed and oscillating square-section cylinders

By P. W. BEARMAN AND E. D. OBASAJU
Department of Aeronautics, Imperial College, London, U.K.

(Received 3 March 1981)

Measurements are presented of the pressure fluctuations acting on a stationary square-section cylinder, with the front face normal to the flow, and one forced to oscillate, transverse to a flow, at amplitudes up to 25 % of the length of a side. The range of reduced velocities investigated, 4–13, includes the vortex lock-in regime. At lock-in the amplification of the coefficient of fluctuating lift is found to be much less than that found for a circular cylinder. The variation of the phase angle, between lift and displacement, is also different from that measured on a circular cylinder, and vortex-induced oscillations are possible only at the high-reduced-velocity end of the lock-in range. At reduced velocities sufficiently far below lock-in the natural vortex-shedding mode is suppressed and vortices are found to form over the side faces at the body frequency. Intermittent reattachment occurs over the side faces and, for an amplitude of oscillation equal to 10 % of the length of a side face, the time-mean drag coefficient can be reduced to 60 % of its fixed-cylinder value.

1. Introduction

Vortex-induced oscillation of a bluff body is an important fluid–structure interaction phenomenon, and many fundamental questions concerning the influence of body movement on the formation and shedding of vortices remain unanswered. The subject has been reviewed most recently by Sarpkaya (1979), where reference to numerous previous investigations can be found. An extraordinary feature of previous work is the enormous effort that has been expended on understanding circular-cylinder flow, with its attendant complex interplay between boundary-layer development and near-wake dynamics. In this paper we examine the flow around a square-section cylinder forced to oscillate at frequencies at and away from its natural vortex-shedding frequency. While much has been written on the subject of vortex-induced oscillation of bluff bodies, comparatively few measurements have been presented of the fluctuating forces experienced by an oscillating body and of the phase during an oscillation cycle at which vortex development induces its maximum lift force. The main emphasis of the work described here is placed on the interpretation of fluctuating-pressure measurements made on an oscillating cylinder.

Spring-mounted square-section cylinders, with one face normal to the flow, are susceptible to the aeroelastic instability known as galloping, and, depending on flow conditions and the mass and mechanical damping of the cylinder, large oscillations can be built up in a direction transverse to that of the stream. At values of n_0/N greater than about 2, where n_0 is the natural vortex-shedding frequency (natural vortex-shedding frequency refers to the frequency that would be measured behind a fixed

cylinder under similar flow conditions) and N the cylinder oscillation frequency, galloping oscillations are well-predicted by quasisteady theory. Quasisteady theory (Parkinson 1974) assumes that the instantaneous lift and drag forces experienced by the cylinder are related to the section's instantaneous incidence and are unaffected by body movement. When n_0/N is near unity galloping and vortex shedding can no longer be considered as separate phenomena, and the quasisteady theory is inapplicable. Wawzonek & Parkinson (1979) have shown that when n_0/N is less than unity galloping oscillations fail to develop, even though quasisteady theory may suggest that they should. The measurements presented here, made over the frequency range $0{\cdot}5 < n_0/N < 2{\cdot}0$, were designed to examine this interesting area. In our experiments a square-section cylinder is forced to oscillate at fixed values of amplitude A over a range of reduced velocity U/ND (and hence n_0/N), where U is the free-stream velocity and D is the section dimension. In forced-oscillation experiments flow parameters can be closely controlled, and ranges of amplitude ratio A/D and reduced velocity examined that would be unobtainable in a free-oscillation experiment. Provided that geometric details, Reynolds number, amplitude ratio and reduced velocity are matched, then flow patterns generated by forced and freely vibrating cylinders should be identical.

Results of experiments on square-section cylinders forced to oscillate transverse to a fluid flow have been reported by Wilkinson (1974), Otsuki *et al.* (1974) and Nakamura & Mizota (1975). Wilkinson presents measurements of mean and fluctuating surface pressure, two-point pressure correlations and the phase angle between the pressure at the centre of a side face and the cylinder displacement. Unfortunately, the accuracy of his fluctuating-pressure measurements was limited by the comparatively long length of tubing he used to connect the surface-pressure tappings to a pressure transducer. An interesting feature of Wilkinson's mean-pressure measurements is that the base suction on the oscillating section is always less than that measured on a stationary one, even in the flow regime where the vortex-shedding frequency locks to the body frequency. In contrast the sectional mean drag on a circular cylinder increases when oscillated, as shown by Sarpkaya (1978), suggesting an increase in the strength of shed vortices. Davies (1976) found that the drag of a D-shaped cylinder also increased when oscillated at vortex resonance, and he detected a substantial increase in vortex strength. Otsuki *et al.* (1974) and Nakamura & Mizota (1975) presented measurements of the fluctuating forces recorded on a length of square-section cylinder about $4{\cdot}5D$ long. As will be discussed in § 4, some correction is required in order to deduce the sectional-force-coefficient behaviour of their oscillating model from the measurements they present.

In the present investigation the characteristics of the surface pressures measured on an oscillating square-section cylinder were examined in detail for a range of amplitude ratio and reduced velocity. In addition to mean and single-point fluctuating pressures, spanwise and chordwise pressure-correlation measurements are described. Measurements of the phase angle between fluctuating pressure and body movement are also presented. The application of the results to the prediction of oscillation amplitudes of a flexibly mounted cylinder are discussed, and comparisons are drawn between the flow characteristics of oscillating circular cylinders and square-section cylinders.

2. Experimental arrangement

The experiments were performed in a low-speed, closed-return wind tunnel with a working section, which was at nominally atmospheric pressure, 0·92 m square and 4·9 m long. The turbulence level in the working section was less than 0·04 %. Three square-section cylinders, spanning the tunnel and each with sides of length 51 mm, were used during the course of the investigation. In the experiments described here the models were mounted with two faces parallel with the direction of the upstream flow and subjected to forced lateral oscillation. The ends of the models protruded through circular holes $3{\cdot}25D$ in diameter in the walls of the tunnel, and were attached to vertical arms connected to an oscillating mechanism beneath the working section. Thin rectangular end plates with rounded corners were attached to the models at 25·4 mm from either wall giving a separation between the plates of $17D$. The end plates, whose effectiveness has been discussed by Obasaju (1979), had dimensions of $6D$ and $4{\cdot}5D$ parallel and perpendicular to the free stream respectively. The front face of the model was $2D$ from the upstream edges of the end plates.

The forced motion of the models was sinusoidal and its frequency could be varied over the range 0 to 20 Hz. The maximum amplitude investigated was about 13 mm, i.e. a maximum amplitude ratio of 0·25. A displacement transducer was used to detect the amplitude of the motion. Further details of the oscillating mechanism are given by Davies (1975). Experiments were conducted with the cylinders stationary and oscillating at amplitude ratios of 0·05, 0·10 and 0·25. The reduced velocity U/ND was varied between 4 and 13, usually by changing U and holding N constant at either 8·6 or 15 Hz. The cylinder Reynolds number varied over the range $5{\cdot}8 \times 10^3$ to $3{\cdot}2 \times 10^4$, and the ratio of Reynolds number to reduced velocity, ND^2/ν, was usually either 1451 or 2531.

One of the models was used to investigate the degree of spanwise uniformity of the time mean flow on the body stationary and oscillating, and a spanwise row of pressure tappings was placed in the rear face. Another of the oscillatory models had eight pressure tappings distributed around its mid-section to measure fluctuating pressures. The remaining model was used for pressure-correlation measurements, and was pressure tapped around the mid-span section and across the span along the centre-line of a side face. The tappings used to measure fluctuating pressures had internal diameters of 1·6 mm.

Fluctuating pressures were measured with $\frac{1}{2}$ in. Setra Pressure Transducers, Model 237, with a range $\pm 0{\cdot}1$ psid. Transducers were mounted inside the models and connected to tappings by tubing of about 2·4 mm internal diameter. The total length of tubing between the surface of the model and the transducer diaphragm was kept below 70 mm, and this gave an approximately flat frequency response up to about 300 Hz. The pressure signal was presented to a low-pass filter set at 300 Hz. Pressure signals were recorded simultaneously with the displacement-transducer signal and analysed on a digital computer. In the case of single-point pressure measurements the data-reduction program provided the power-spectral density of the pressure and displacement signals, the coherence between the two, and the average value of the phase difference between the displacement and that part of the pressure signal that was at the cylinder frequency. Cross-correlation and cross-power-spectral density information was obtained for two-point pressure measurements. Unless stated, none of the results

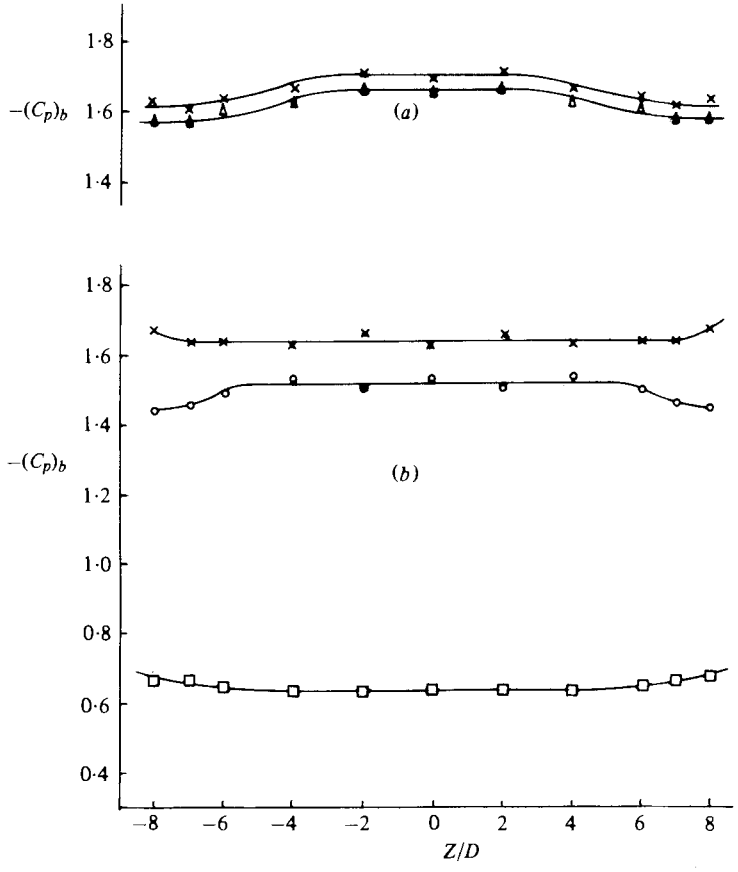

FIGURE 1. Distribution of base-pressure coefficient across model span. (*a*) $Re = 4{\cdot}7 \times 10^4$: ×, $A/D = 0$; △, $A/D = 0{\cdot}10$, $U/ND = 17{\cdot}9$. (*b*) $Re = 1{\cdot}1 \times 10^4$: ×, $A/D = 0$; □, $A/D = 0{\cdot}10$, $U/ND = 4{\cdot}3$. $Re = 1{\cdot}9 \times 10^4$: ○, $A/D = 0{\cdot}10$, $U/ND = 7{\cdot}1$.

presented have been corrected for the effects of wind-tunnel blockage. The geometric blockage was about 5·5 %, and on the fixed cylinder the correction required to velocity, according to the method of Maskell (1963), would be about 5 %. However, there is insufficient information available on how best to correct fluctuating pressure measurements or measurements made with oscillating bluff bodies.

3. Experimental results

3.1. *Two-dimensionality of the mean flow*

Initially, measurements were made to examine the uniformity of base pressure along the cylinder span. Some of the results are presented in figure 1, where the mean base-suction coefficient measured on the centre-line of the back face $-(C_p)_b$ is plotted against the distance z/D from the centre span for the model held stationary, i.e. $A/D = 0$, and for the model oscillating with an amplitude of $0{\cdot}1D$. The results indicate that, on the stationary model, the extent of the span over which the base pressure is uniform is smaller at the higher Reynolds number. The influence of body motion is to reduce the base suction, the magnitude of the reduction depending on the reduced

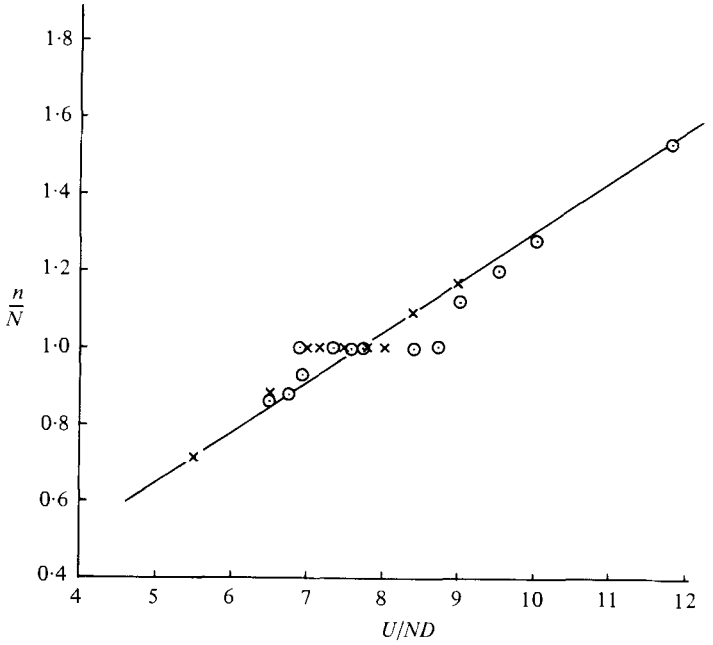

FIGURE 2. Vortex-shedding frequency versus reduced velocity.
——, $A/D = 0$; ×, 0·05; ○, 0·10.

velocity. Two-point pressure correlations (to be presented in § 3.4), with the two points separated in the spanwise direction, were measured in the Reynolds-number range from 7×10^3 to $1{\cdot}8 \times 10^4$. For this range, mean-pressure measurements indicated that the base pressure was uniform over at least the centre 70 % of the span. Single-point fluctuating-pressure measurements on the oscillating models were taken at the centre span for Reynolds numbers in the range from $5{\cdot}8 \times 10^3$ to $3{\cdot}2 \times 10^4$.

3.2. *Vortex-shedding-frequency measurements*

The vortex-shedding frequency n was estimated from power spectra of pressure fluctuations recorded at the centre of a side face of the square section: n, divided by body frequency N, is shown plotted in figure 2 against reduced velocity. The line drawn in figure 2 represents the shedding frequency of the stationary model, and hence the reduced velocity at which $n/N = 1$ is equal to the inverse of the stationary-body Strouhal number. This reduced velocity, which will be referred to as the resonance point, has a value of 7·7 and gives a Strouhal number of 0·13. This Strouhal number is in close agreement with that found by Bearman & Trueman (1971).

Pressure spectra measured on the oscillating body show differing characteristics depending on whether or not the shedding frequency is captured by the body frequency. Away from lock-in, peaks occur not only at the shedding and body frequencies but also at harmonics and combinations of these frequencies. Peaks at the sum and difference of the body and shedding frequencies are particularly dominant. In the lock-in range only harmonics of the body frequency are seen and the outstanding peak is the one at the fundamental. Spectra with similar features were obtained from hot-wire signals recorded from a probe positioned outside the wake at about $3D$ downstream of the

cylinder. The lock-in region spanned the range $7{\cdot}0 \leqslant U/ND \leqslant 8{\cdot}0$ for $A/D = 0{\cdot}05$ and $6{\cdot}9 \leqslant U/ND \leqslant 8{\cdot}7$ for $A/D = 0{\cdot}10$. At the highest amplitude examined, $A/D = 0{\cdot}25$, peaks associated with the body frequency were so large that it was difficult to identify a separate shedding frequency, particularly at low values of U/ND, where the body frequency is higher than the natural shedding frequency. Although not plotted in figure 2 it is estimated that for $A/D = 0{\cdot}25$ the lock-in range extended up to about $U/ND = 12$. Vortex shedding at low values of reduced velocity is discussed further in § 4.

3.3. *Mean-pressure measurements*

Mean pressures around the square-section cylinder were measured for a range of amplitudes and reduced velocities, and presented as pressure coefficients. Figure 3 shows a selection of pressure distributions taken in the lock-in region for $A/D = 0{\cdot}1$ and $0{\cdot}25$, together with results for the stationary model. Oscillation was found to have a very small effect on the front-face pressures and, therefore, any changes in drag coefficient will be reflected by changes in base pressure. The base-pressure coefficient $(C_p)_b$, measured at the centre of the base, is shown plotted in figure 4 against reduced velocity for $A/D = 0{\cdot}1$. As a comparison $(C_p)_b$ for the stationary model is shown on the same figure, and the variation with U/ND here represents only the effect of changing Reynolds number, since $U/ND = (UD/\nu)/(ND^2/\nu)$, and the value chosen for ND^2/ν is the same as that used for the oscillating-body experiments. The sharply rising base pressure seen on the oscillating model as reduced velocity is decreased below about 7 indicates a substantial reduction in drag. At $U/ND = 4$ and $A/D = 0{\cdot}1$ the cylinder mean drag is about half of its stationary-cylinder value. Figure 4 shows a distinct peak in base suction at a reduced velocity slightly less than the resonant value (i.e. 7·3 rather than 7·7). On the oscillating section, base suction never exceeded that measured on the stationary model at a similar Reynolds number, and at the highest amplitude tested, $A/D = 0{\cdot}25$, the peak in suction broadened slightly and was centred on about $U/ND = 7{\cdot}0$. These observations on the effect of body movement on base suction are in general agreement with mean-pressure measurements made by Wilkinson (1974) on an oscillating square-section cylinder.

3.4. *Fluctuating-pressure measurements*

Fluctuating pressures were measured on the stationary and oscillating models and are presented as pressure coefficients C'_p, where C'_p is defined as $p'_{\mathrm{rms}}/\frac{1}{2}\rho U^2$, and p'_{rms} is the root-mean-square value of the pressure fluctuations. In figure 5 the distribution of fluctuating pressure on the stationary model is shown compared with measurements of Vickery (1966), Pocha (1971), Lee (1975) and Wilkinson (1974). In preparing figure 5 we made some allowance for the different experimental conditions under which the various investigators obtained their results, by correcting the free-stream dynamic pressure for the effect of tunnel blockage by the method of Maskell (1963). Pocha's results are presented unaltered as his experiments were carried out in an open jet, and Vickery's are unchanged as his results were already corrected. In spite of these corrections the scatter between the results of the various authors is considerable. Some of this scatter may be attributable to the effect of Reynolds-number differences, since we found (see figure 6) that increasing Reynolds number

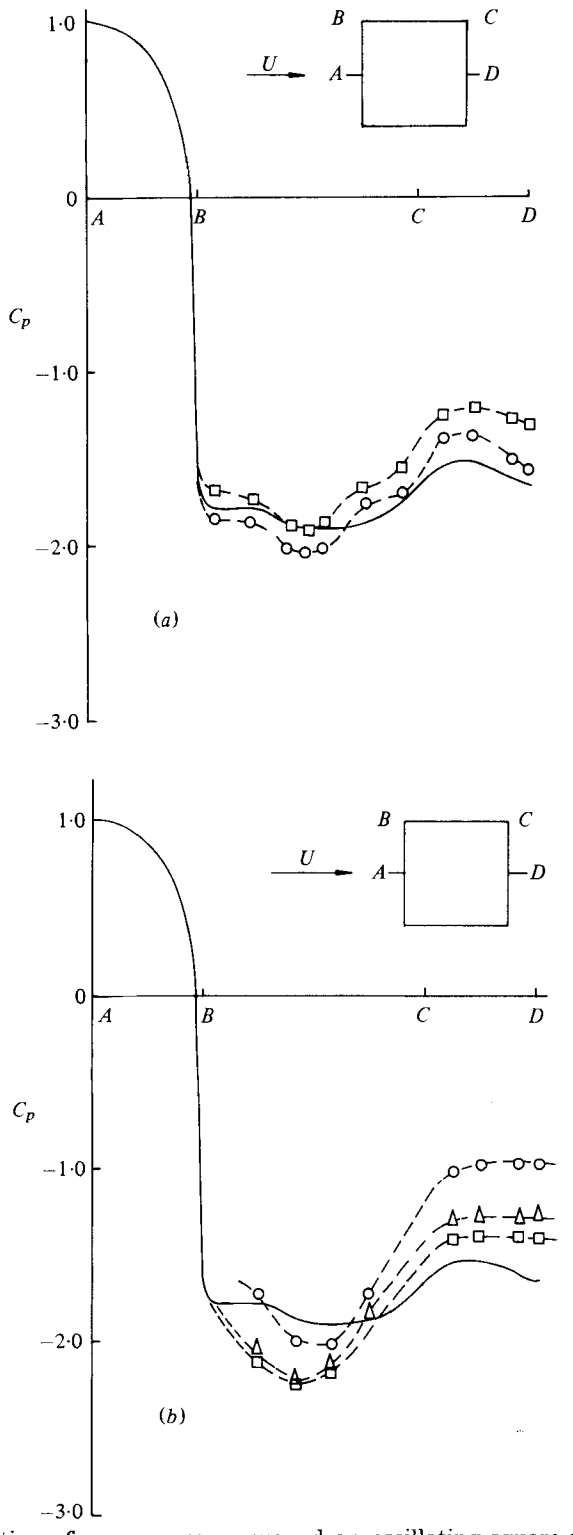

FIGURE 3. Distribution of mean pressure around an oscillating square-section cylinder. ——, $A/D = 0$. (*a*) $A/D = 0{\cdot}10$: ○, $U/ND = 7{\cdot}5$; □, 8·4. (*b*) $A/D = 0{\cdot}25$: □, $U/ND = 7{\cdot}5$; △, 7·8; ○, 8·5.

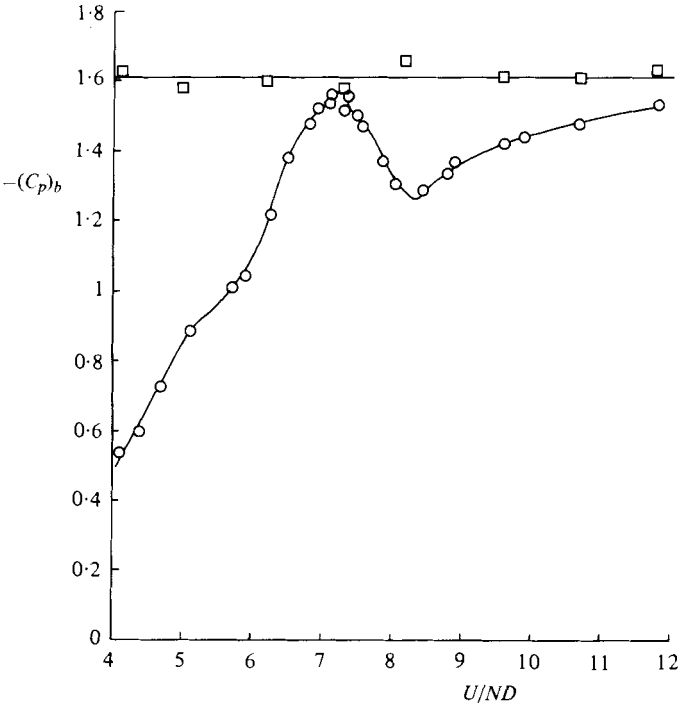

FIGURE 4. Base-pressure coefficient versus reduced velocity. □, $A/D = 0$; ○, 0·10.

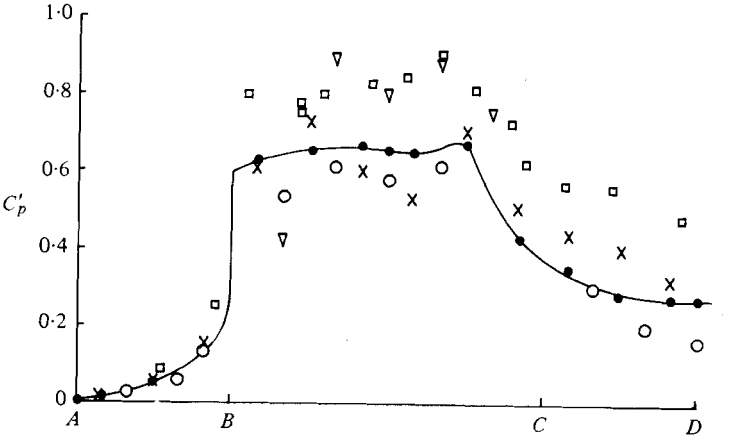

FIGURE 5. Distribution of fluctuating pressure on a stationary square-section cylinder. ●, Present results, $Re = 2 \times 10^4$; ×, Lee (1975), $Re = 1{\cdot}76 \times 10^5$; □, Pocha (1971), $Re = 9{\cdot}2 \times 10^4$; ▽, Vickery (1966), $Re = 4 \times 10^4$–$1{\cdot}6 \times 10^5$; ○, Wilkinson (1974), $Re = 10^4$–10^5.

raised C'_p on the rear face, although it had little effect on the side-face fluctuating pressures. The results presented in figure 5, however, show no consistent trend with Reynolds number. Another possibility is that the results are influenced by the aspect ratio of the models tested.

Measurements of the correlation of pressure over the side faces, to be described later, were used in conjunction with the fluctuating pressure measurements to estimate the

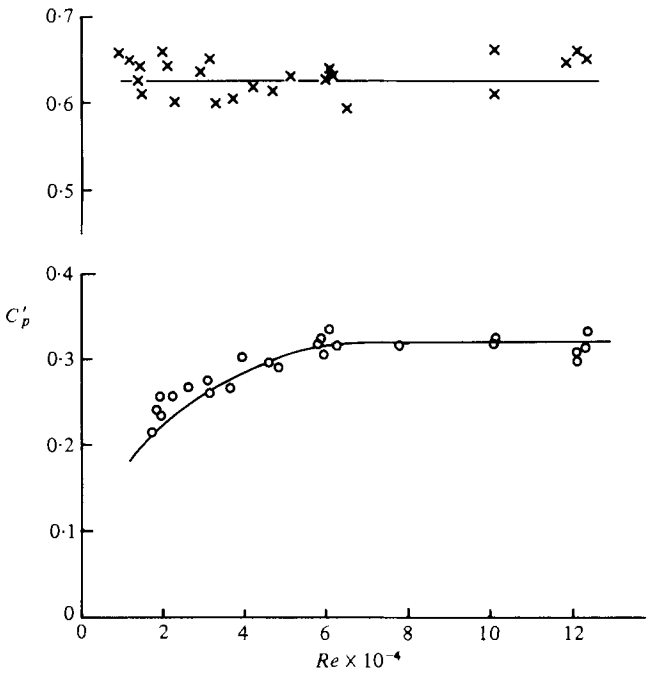

FIGURE 6. Effect of Reynolds number on fluctuating pressure measured with the model stationary. ×, centre of side face; ○, centre of rear face.

r.m.s. value of the sectional fluctuating lift coefficient $C_{\mathrm{L\,rms}}$, defined as r.m.s. lift per unit length, divided by $\frac{1}{2}\rho U^2 D$. With allowance for blockage, our value of $C_{\mathrm{L\,rms}}$ is about 1·2, while the values reported by the other workers whose results are presented in figure 5 range from 1·2 to 1·4.

Measurements of fluctuating pressure on the oscillating model were made with the pressure transducer mounted inside the model. Ideally the pressure transducer should be mounted flush with the cylinder surface, but the comparatively large size of the transducer dictated that it had to be mounted along the central axis of the model and connected to a surface pressure hole by a short length of tubing. Bearman & Currie (1979) have discussed how this leads to a spurious pressure signal at the body frequency if the model experiences any acceleration along a line connecting the transducer to the surface-pressure hole. The r.m.s. pressure coefficient due to this effect, $C'_{p\mathrm{A}}(N)$, is given by

$$4\sqrt{2}\,\pi^2 \frac{A}{D}\frac{h}{D}\left(\frac{ND}{U}\right)^2,$$

where in our case h is the perpendicular distance between a side face and the centre of the transducer diaphragm. Measurements of C'_p can be corrected for the effect of tube length by using the relation

$$C'_p = (C'^2_{p\mathrm{A}}(N) + C'^2_{p\mathrm{m}} - 2C'_{p\mathrm{A}}(N)\,C'_{p\mathrm{T}}(N)\cos\beta)^{\frac{1}{2}}, \tag{1}$$

where $C'_{p\mathrm{m}}$ is the measured fluctuating pressure coefficient, β is the measured phase angle by which suction leads the displacement, and $C'_{p\mathrm{T}}(N)$ is the measured r.m.s. value

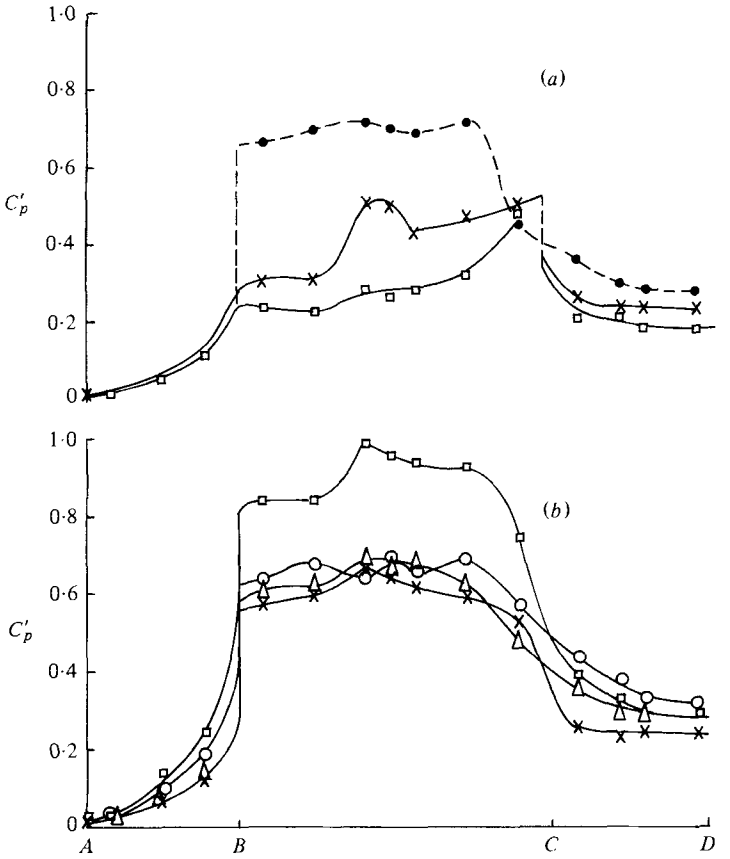

FIGURE 7. Distribution of fluctuating pressure on an oscillating square-section cylinder. (*a*) ●, $A/D = 0$; □, $A/D = 0{\cdot}10$, $U/ND = 6{\cdot}2$; ×, $A/D = 0{\cdot}10$, $U/ND = 6{\cdot}5$. (*b*) $A/D = 0{\cdot}10$: ○, $U/ND = 7{\cdot}0$; □, 7·8; ×, 8·7; △, 12·0.

of the component of the fluctuating pressure at the cylinder oscillation frequency. Measured phase angles can be corrected by the relation

$$\phi = \arctan\left(\frac{C'_{p\mathrm{T}}(N)\sin\beta}{C'_{p\mathrm{T}}(N)\cos\beta - C'_{p\mathrm{A}}(N)}\right). \tag{2}$$

The phase angle ϕ is chosen to be the angle by which suction, or pressure less than the mean, leads displacement, since suction is expected to be closely in phase with lift. All measurements of phase angles presented in this paper have been corrected according to (2). Most of the measurements of fluctuating pressure were not corrected for the acceleration effect, but since the majority of the measurements reported here were made at an amplitude of $0{\cdot}1D$ the correction will be small, except at low values of reduced velocity. The magnitude of the correction depends on the phase angle and at worst in the lock-in range it could rise to 4 %, but it is typically about 2 %. At the lowest value of U/ND investigated, 4·1, the error is more serious and rises as high as 20 %. Therefore, the values of C'_p at low reduced velocities need to be treated with caution. The fluctuating pressures shown in figures 9 and 10 were corrected, however.

Distributions of fluctuating pressure are presented in figure 7 for $A/D = 0{\cdot}1$ and for

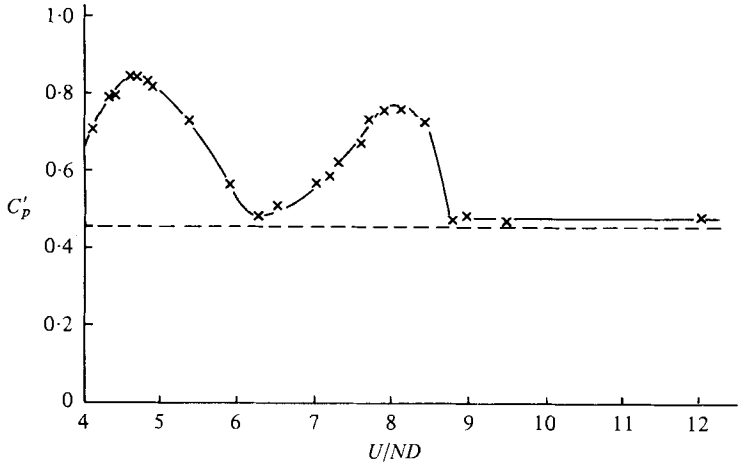

FIGURE 8. Fluctuating pressure measured on a side face, at $0{\cdot}49D$ from a front corner, versus reduced velocity. – – – –, $A/D = 0$; ×, 0·10.

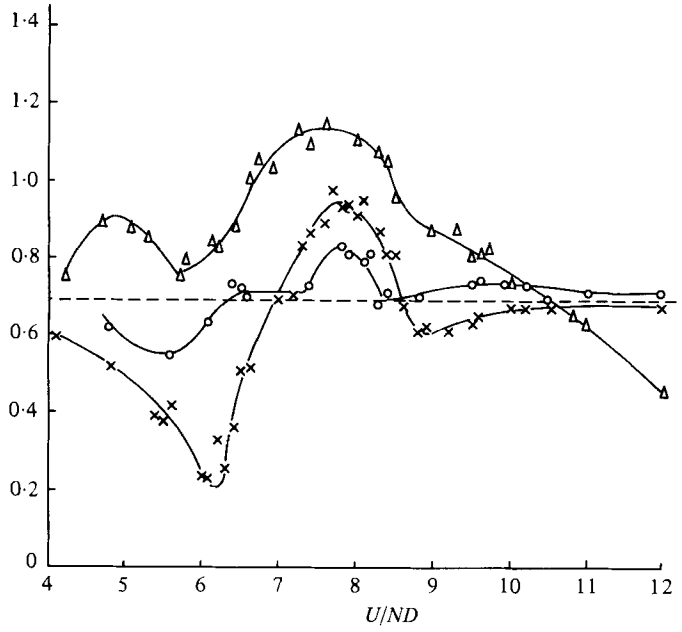

FIGURE 9. Effect of amplitude and reduced velocity on the fluctuating pressure measured at the centre of a side face. – – – –, $A/D = 0$; ○, 0·05; ×, 0·10; △, 0·25.

selected values of U/ND in the range 6·2–12·0. The level of fluctuating pressure varies through the lock-in range, with the largest values of C'_p occurring at $U/ND = 7{\cdot}8$, i.e. close to the resonance point. On the rear face, maximum fluctuating pressures occur at a lower value of U/ND, about 7·3, where figure 4 shows the mean base suction and drag to be a maximum. At reduced velocities above lock-in, where the natural shedding frequency is higher than the body frequency, the fluctuating-pressure levels are generally similar to those measured on the fixed model. On the other hand, the distributions of fluctuating pressure measured at reduced velocities below lock-in show a

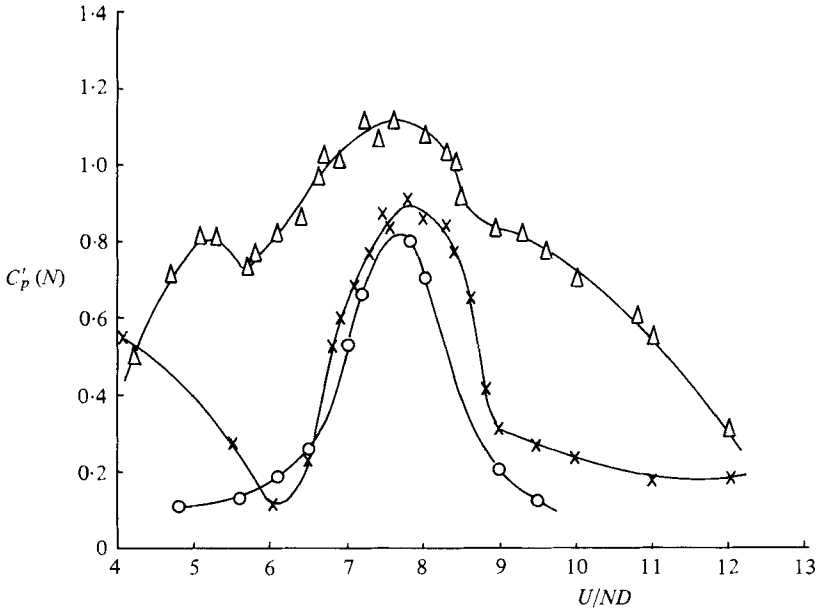

FIGURE 10. Effect of amplitude and reduced velocity on fluctuating pressure, at the body frequency, measured at the centre of a side face. ○, A/D = 0·05; ×, 0·10; △, 0·25.

distinctive rise in C'_p towards the rear corners. Fluctuating pressures measured at a point near a trailing-edge corner are shown plotted in figure 8 against reduced velocity. In addition to the peak in the normal vortex lock-in range a second peak occurs, centred on about U/ND = 4·8. The possibility that this peak could be due to resonance with a second mode of shedding associated with vortices forming, at the body frequency, in the shear layers over the side faces, is discussed in § 4.

For the amplitude ratios tested, figure 9 shows the variation with reduced velocity of the coefficient of fluctuating pressure measured at the centre of a side face. Corresponding values of the component of the fluctuating pressure at the body frequency, $C'_p(N)$, are presented in figure 10. It can be seen from figures 9 and 10 that increasing oscillation amplitude raises the fluctuating pressure levels in the lock-in range, and that peak values of C'_p remain centred on a reduced velocity of about 7·8. At values of U/ND above the resonance point the curves in figure 9 show a characteristic dip before returning to approximately the stationary cylinder value at high U/ND. It seems likely that if the results for A/D = 0·25.were taken to higher values of U/ND they would show a similar trend. At reduced velocities below resonance the fluctuating pressures for the higher amplitudes are dominated by fluctuations at the body frequency.

In order to estimate the sectional coefficient of fluctuating lift, measurements of the correlation of the pressures across the side faces were required. The side-face pressure tappings were connected in turn to a pair of pressure transducers within the model, and a matrix of pressure correlation coefficients were measured. Their values for the stationary model are shown in figure 11 (*a*), where it can be seen that they are generally close to unity. Slightly lower correlations were measured when one transducer was located near a trailing-edge corner. This lower correlation near a trailing corner was more marked on the oscillating model, and figure 11 (*b*) shows pressure correlations in the lock-in range for U/ND = 7·9 and A/D = 0·1. Also shown in the figure are some

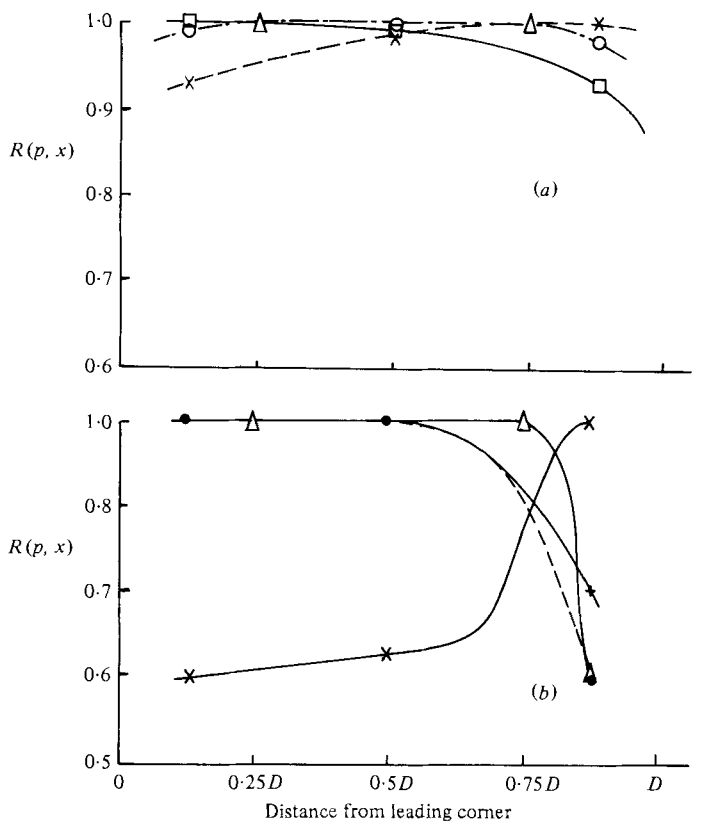

FIGURE 11. Correlation between pressures measured on a side face. (*a*) Cylinder stationary: ○, reference transducer at $X/D = 0{\cdot}5$; ×, 0·875; □, 0·125; △, 0·25. (*b*) Cylinder oscillating; $A/D = 0{\cdot}10$: ●, reference transducer at $X/D = 0{\cdot}125$; △, 0·25; ×, 0·875; +, $A/D = 0{\cdot}25$; $X/D = 0{\cdot}125$.

pressure correlations for $A/D = 0{\cdot}25$, and these show equally high values. Using these correlations and measurements of fluctuating pressure, coefficients of fluctuating lift $C_{\mathrm{L\,rms}}$ can be estimated. Figure 12 shown $C_{\mathrm{L\,rms}}$, uncorrected for blockage, plotted against A/D for $U/ND = 7{\cdot}8$.

To complete the pressure data, measurements were made of the spanwise correlation of fluctuating pressure along a line coinciding with the centre-line of a side face. Results for $A/D = 0{\cdot}1$ are presented in figure 13, where the correlation coefficient $R(p, z)$ is plotted against spanwise separation z/D for several values of U/ND. Measured values of $R(p, z)$ have not been corrected for the acceleration effect mentioned earlier, but for $A/D = 0{\cdot}1$ it is not thought that correction would affect the results significantly. Spanwise correlation measurements on the stationary cylinder, which give a spanwise correlation length of $5{\cdot}6D$, are in agreement with the results of Vickery (1966), Pocha (1971) and Lee (1975). By comparison, the oscillating-model results show much higher correlation, particularly around the resonance point, where a correlation coefficient of 0·9 was recorded at the maximum separation of $13{\cdot}25D$. Such high correlation was also observed for $A/D = 0{\cdot}05$, where any spurious correlation due to the positioning of the pressure transducers can be neglected.

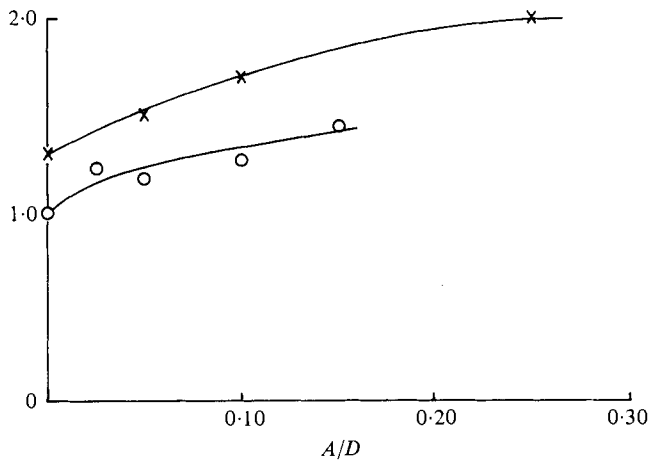

FIGURE 12. Coefficient of fluctuating lift, measured in the vortex lock-in region, versus amplitude ratio. ×, present results estimated from fluctuating pressure. ○, results of Nakamura & Mizota (1975) estimated from total force measurements.

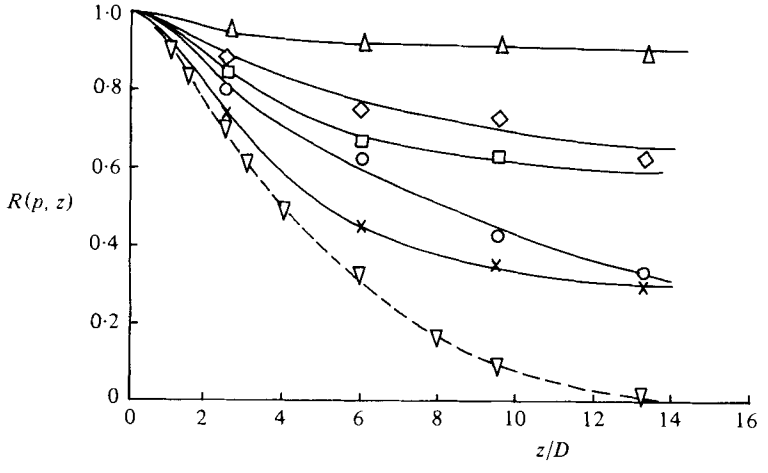

FIGURE 13. Correlation of surface pressures, measured on the centre-line of a side face, versus spanwise separation. ▽, $A/D = 0$. $A/D = 0{\cdot}10$: ×, $U/ND = 6{\cdot}2$; ○, 7·0; □, 12·0; ◇, 8·8; △, U/ND within the range 7·3–8·5.

3.5. *Phase-angle measurements*

Measurements of the phase angle ϕ by which the suction at the centre of a side face leads the displacement, are plotted in figure 14 against reduced velocity. If the lift force on the cylinder is to be capable of sustaining oscillations of a spring-mounted cylinder, then this phase angle needs to be within the range $0° < \phi < 180°$. For $A/D = 0{\cdot}05$ and 0·1, figure 14 shows that the phase angle exhibits discontinuities at the two ends of the lock-in range and that ϕ changes by more than 150° through this range. Assuming a similar behaviour for the highest-amplitude case of $0{\cdot}25D$ it can be deduced that lock-in probably occurs over the range $5{\cdot}5 < U/ND < 12$. These measurements will be discussed further in § 4.

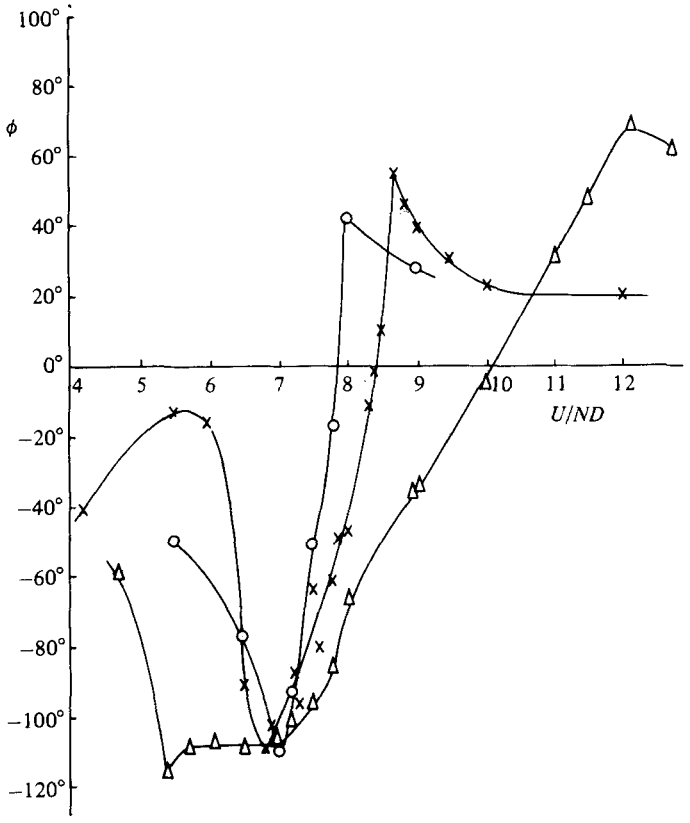

FIGURE 14. Measurements of the phase angle between suction, measured at the centre of a side face, and cylinder displacement. ○, A/D = 0·05; ×, 0·10; △, 0·25.

4. Discussion of results

As in the case of an oscillating circular cylinder, the characteristics of the flow around an oscillating square-section cylinder are dependent on reduced velocity and amplitude ratio. Three distinct flow regimes can be identified; vortex lock-in, above lock-in and below lock-in. At reduced velocities above lock-in, where the natural shedding frequency is higher than the body frequency, the flow approaches a quasisteady form. Below lock-in the flow is dominated by the effects of the imposed oscillation, and, depending on oscillation amplitude, concentrated vorticity is generated and shed at the body frequency, and the natural vortex-shedding mode can be completely suppressed. The lock-in regime is defined as the reduced velocity range, about the resonant point, where the natural vortex-shedding frequency transfers to the body frequency. It is only in the lock-in range that a flexibly mounted square-section cylinder can be expected to undergo vortex-induced oscillations.

Very few measurements have been published of the forces acting on oscillating square-section cylinders. Otsuki *et al.* (1974) and Nakamura & Mizota (1975) have measured what they term the 'frequency-response' component of the lift force acting on a square section forced to oscillate transversely to an air stream. They also measured the phase angle of the component relative to the displacement of the model. Their frequency-response lift coefficient is defined as the r.m.s., of the component at the body

frequency, of the quantity $(F_L(t) - V(t))/(\frac{1}{2}\rho U^2 DW)$, where W is the length of the cylinder. $F_L(t)$ and $V(t)$ are measured side forces on a cylinder oscillated in a uniform stream and an identical cylinder oscillated in still air. Subtracting $V(t)$ from $F(t)$ conveniently removes the force due to the inertia of the model, but $V(t)$ also includes a contribution due to the aerodynamic force developed by a cylinder oscillating in still air. Bearman & Graham (1979) have shown that the force acting on a square-section cylinder oscillating at small amplitude in still fluid can be approximated by the expression

$$\tfrac{1}{4}\rho\pi D^2 W \frac{d^2y}{dt^2} C_m,$$

where d^2y/dt^2 is the acceleration of the cylinder and C_m is the inertia coefficient, which takes a value of about 2·8. We have corrected the results of Otsuki *et al.* and of Nakamura & Mizota to make allowance for the aerodynamic force acting on the cylinder oscillating in still air.

A comparison between our own estimates of the r.m.s. lift coefficient in the lock-in range and the r.m.s. of the frequency response component of Nakamura & Mizota is shown plotted in figure 12. At each value of amplitude ratio the coefficient plotted is the highest value recorded through the lock-in range. On the stationary cylinder the result recorded due to Nakamura & Mizota is the r.m.s. of the total lift acting on the cylinder. Compared with our values, those of Nakamura & Mizota are generally about 20 % lower, the correction mentioned above reducing their results by at most 3 %. It is reasonable that their cylinder result should be less than ours, since they integrated forces over a length of cylinder equal to about 4·7D. However, at the highest amplitude completely correlated flow can be expected and the difference in the results may be due to details of the experimental arrangements. The tunnel blockage is similar in both experiments, but the aspect ratios of the cylinders used are 4·7 and 17, and this may influence fluctuating lift values. Phase-angle results are plotted in figure 15 for an amplitude ratio of 0·1. The data of Otsuki *et al.* and Nakamura & Mizota are shown, both corrected and uncorrected, and it can be seen that the correction does not substantially change the form of the results. Although the shape of all three curves is similar, the detailed agreement is poor; for example there is a spread of more than 15 % in the value of reduced velocity at which the phase angle passes through zero.

Compared with the circular cylinder, the square-section cylinder does not show such a spectacular increase in fluctuating lift in the lock-in range as the amplitude of oscillation is increased. Bearman & Currie (1979) show that for a circular cylinder the r.m.s. coefficient of fluctuating pressure, measured at a position 90° round from the front mean stagnation point, increases some three and a half times at lock-in as the amplitude of oscillation is raised to 0·22D. At a similar amplitude the present results show about a 60 % increase in r.m.s. pressure fluctuations on a side face. Figure 16 shows samples of the pressure signal recorded in the centre of a side face for the stationary model and for the model oscillating at an amplitude ratio of 0·1. A feature of the stationary cylinder pressure trace, shown in figure 16(*a*), is the amplitude modulation of the narrow-band shedding signal. Further details of the modulation can be seen in figure 17, where the outputs of two pressure transducers are displayed. With the transducers at the same spanwise station, but on opposite faces, the modulation is seen to be in phase (figure 17*a*). Figure 17(*b*), however, shows that when the transducers are on the same face, displaced apart a spanwise distance of 2·5D, the

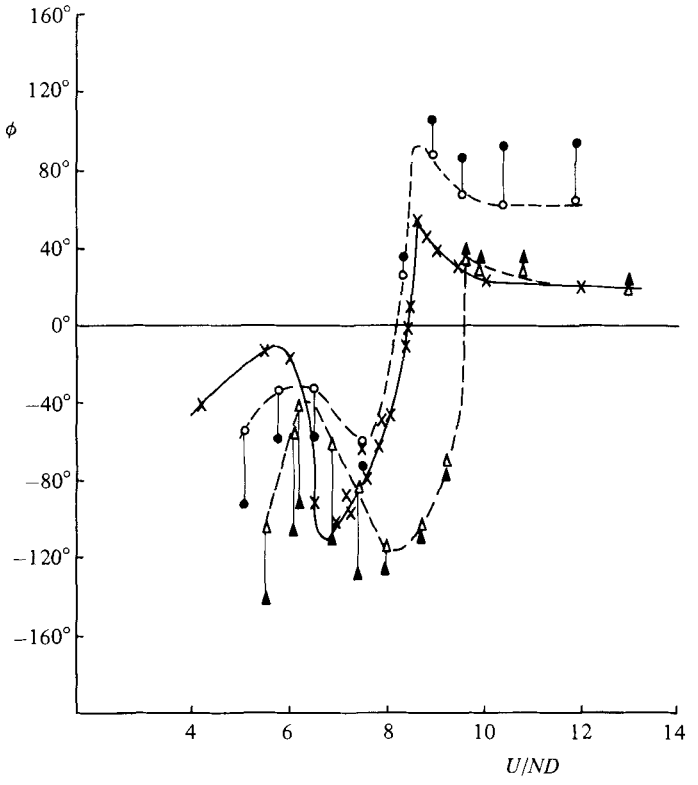

FIGURE 15. Phase angle versus reduced velocity for $A/D = 0{\cdot}10$. ×, present results. Data of Otsuki *et al.* (1974): ●, as presented; ○, corrected. Data of Nakamura & Mizota (1975): ▲, as presented; △, corrected.

modulation is no longer always in phase. Hence the modulation seems to be related to local changes in the vortex-shedding structure.

Returning to figure 16, it is seen that the character of the pressure signal on the oscillating model depends strongly on reduced velocity. In the lock-in range (figure 16*c*) the signal is less modulated than that for the stationary cylinder, but maxima in peak-to-peak pressure fluctuations are little different. Thus it is observed that the increase in the r.m.s. pressure-fluctuation level with oscillation can be attributed to the more organized periodic nature of the shedding. Below lock-in, at a reduced velocity of 6·26 (figure 16*b*), the pressure fluctuation level is considerably weaker, and above lock-in (figure 16*d*) a beating between the body frequency and the shedding frequency is clearly seen.

When a square section is oscillated, a number of mechanisms may generate pressure fluctuations on the side faces: vortex shedding, pressure fluctuations linked directly to the acceleration of the body, and pressure fluctuations due to the continual variation of the angle of incidence of the cylinder. At low-enough values of U/ND, pressure fluctuations resulting from the inertia of the fluid will dominate, but within the lock-in range pressure fluctuations due to vortex shedding have the major influence. Evidence to justify this latter statement is provided by the measurements of the phase angle ϕ (figure 14), which show an extremely large phase change through lock-in, at least 150°. This is caused by the vortices as they adjust their point of formation and

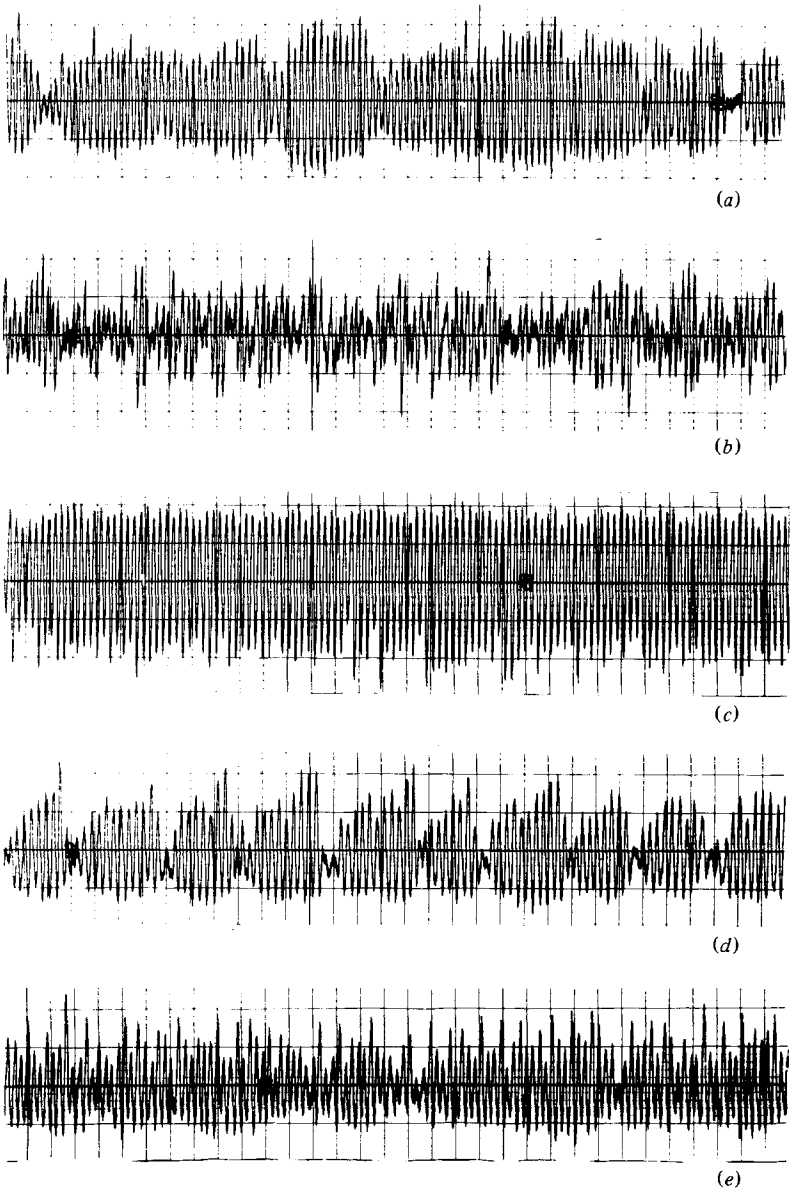

FIGURE 16. Traces of the pressure signal measured at the centre of a side face. (*a*) $A/D = 0$, $C_{p\text{rms}} = 0{\cdot}71$. $A/D = 0{\cdot}10$: (*b*) $U/ND = 6{\cdot}3$, $C_{p\text{rms}} = 0{\cdot}33$; (*c*) 7·8, 0·97; (*d*) 9·0, 0·60; (*e*) 12·0, 0·70.

shedding through the lock-in range. At the low-reduced-velocity end of lock-in the lift is a maximum positive, positive upwards, as the cylinder is passing downwards approximately through its mean position. At the high-velocity end of lock-in the lift maximum occurs as the body is moving upwards towards its maximum displacement. For vortex-induced oscillations to occur on a flexibly mounted cylinder the phase angle must be between 0° and 180°, and it can be seen that this only occurs towards the high-reduced-velocity end of lock-in.

Considerable progress has been made in predicting the response due to vortex

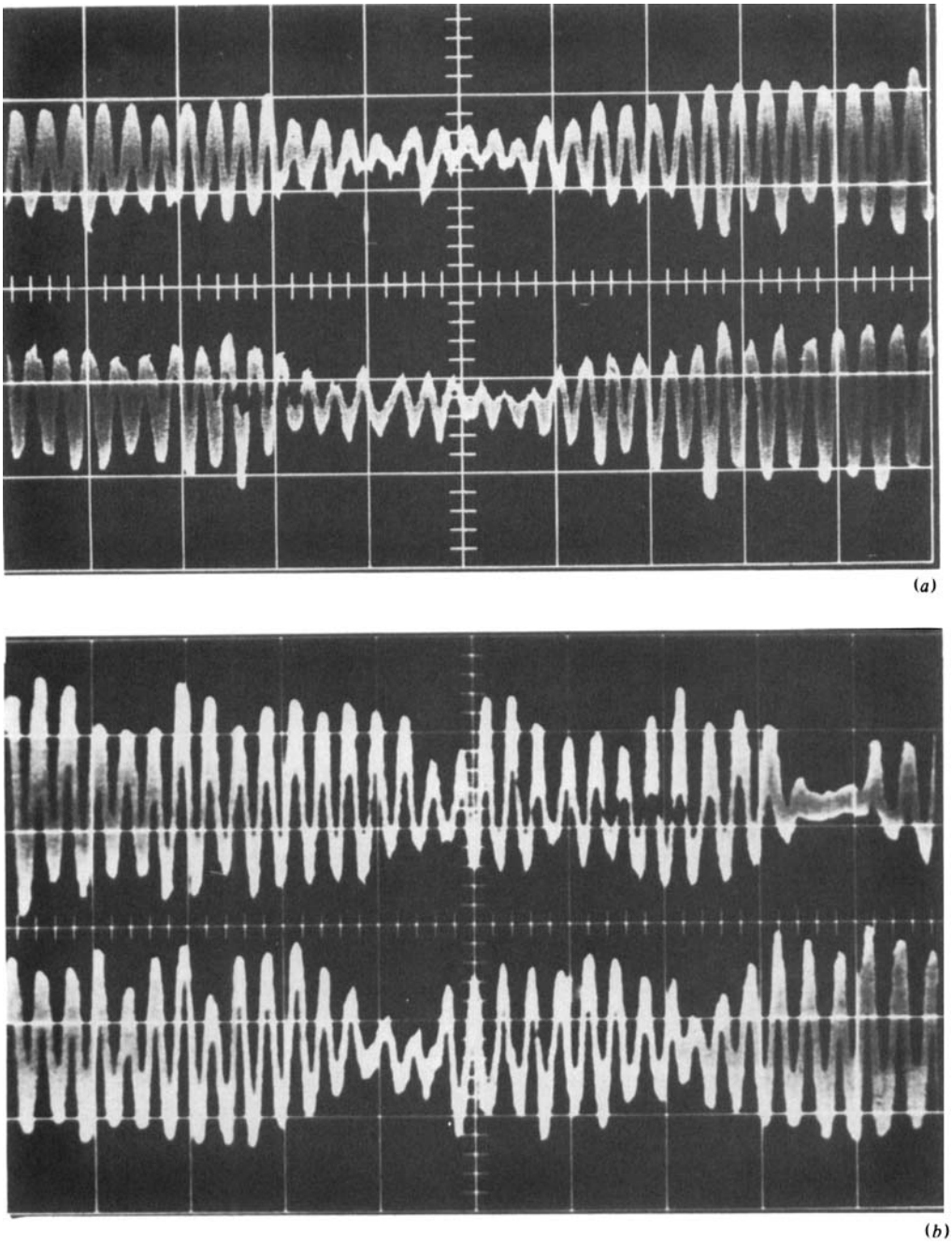

FIGURE 17. Sample traces from two pressure transducers located on the side faces of a stationary square-section cylinder. (*a*) In the centres of opposite faces at the same spanwise position, $R(p,x) = -0{\cdot}96$. (*b*) Both transducers at mid-chord on the same face with a spanwise separation of $2{\cdot}5D$.

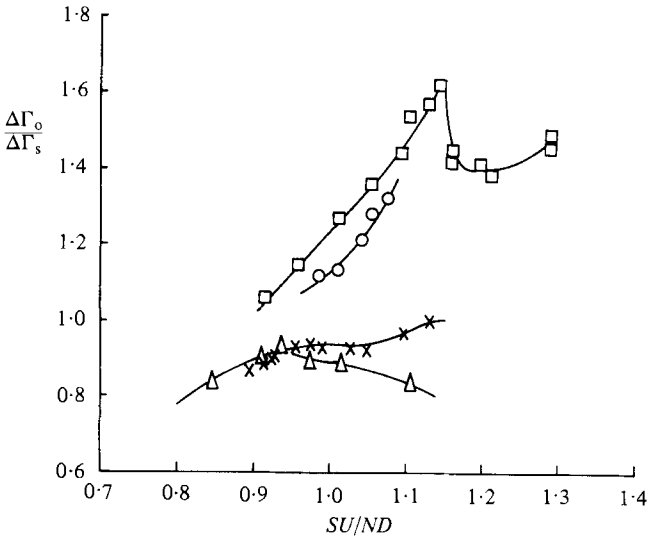

FIGURE 18. Circulation shed per cycle in the vortex lock-in regime versus SU/ND. Square-section cylinder: ×, A/D = 0·10; △, 0·25. Circular cylinder: ○, A/D = 0·10; □, 0·29.

shedding of flexibly mounted circular cylinders, using mathematical models such as that suggested by Hartlen & Currie (1970), based on nonlinear oscillator theory. It is instructive, therefore, to compare some of our measurements made in the lock-in regime with those for a circular cylinder. Results for both sections show that oscillation produces a marked increase in the spanwise correlation of fluctuating flow properties. Tanida, Okajima & Watanabe (1973) and Stansby (1976) have shown that the coefficient of mean drag and the base suction of a circular cylinder are both increased during lock-in. The largest amplification occurs towards the upper end of the lock-in range, above the resonant reduced velocity. Bishop & Hassan (1964*a*, *b*) have reported large increases in the fluctuating lift and drag of oscillating circular cylinders. These changes in sectional characteristics are assumed to be due to increased vortex strength. The mean rate of shedding of circulation from a separation point of a bluff body is given approximately by $\frac{1}{2}(1-C_{pb})\,U^2$ (Roshko 1954). Hence the circulation shed during the formation of a vortex $\Delta\Gamma/UD$ is $\frac{1}{2}(1-C_{pb})\,(U/nD)$. As discussed by Roshko (1954), the strength of the vortices discharged into the wake will be substantially less than this, because approximately 50 % of the vorticity is cancelled in the near wake by mixing with vorticity of opposite sign from the opposing shear layer. The ratio of circulation shed from an oscillating body to that shed by a stationary body $\Delta\Gamma_o/\Delta\Gamma_s$ is given approximately by the relation $((1-C_{pb})_o/(1-C_{pb})_s)\,SU/ND$, where S is the stationary-body Strouhal number and the suffix o refers to oscillating and s to stationary. $\Delta\Gamma_o/\Delta\Gamma_s$ is plotted against SU/ND in figure 18 for both a circular cylinder and a square-section cylinder; the quantities for a circular cylinder have been deduced from the measurements of Stansby (1976). This figure demonstrates that the circulation shed per cycle is substantially amplified for a circular cylinder during lock-in, whereas the square-section cylinder shows a slight attenuation.

In addition to these differences in the shed circulation there are also differences between the two bodies in the way the phase angle between lift and displacement varies

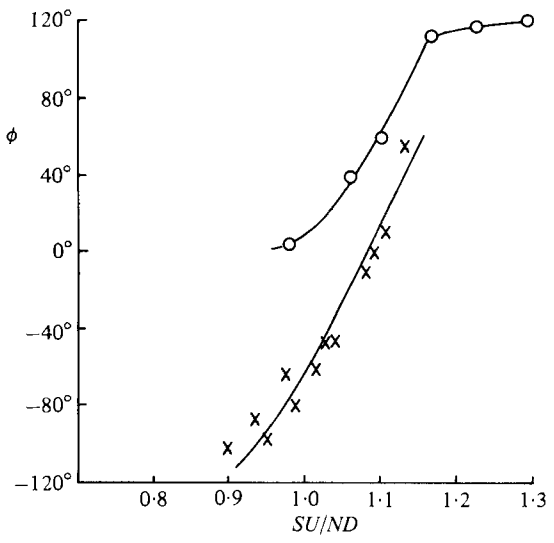

FIGURE 19. Variation through lock-in of the phase angle between surface suction and cylinder displacement. ×, $A/D = 0{\cdot}11$; square-section cylinder, pressure-measuring point at the centre of a side face. ○, $A/D = 0{\cdot}11$; circular cylinder, pressure-measuring point at 90° from the front stagnation point (Bearman & Currie 1979).

through lock-in. Figure 19 shows a comparison between the phase of the pressure fluctuations at 90° on a circular cylinder oscillating at an amplitude ratio of 0·11, taken from the work of Bearman & Currie (1979), and the phase of the fluctuating pressure at the centre of a side face of a square section oscillating at $A/D = 0{\cdot}1$. As mentioned earlier, for a spring-mounted bluff body to develop vortex-induced oscillations this phase angle must be positive. It can be seen from figure 19 that, whereas the circular cylinder has the possibility of sustaining oscillations over the whole of the lock-in region, vortex-induced oscillation of a square section is limited to a small reduced-velocity range at the upper end of lock-in. Summarizing our findings, we observe that the fluctuating lift coefficient on a square-section cylinder is greater than values reported for a circular cylinder at a sub-critical Reynolds number when both are stationary, but body oscillation amplifies the lift on a circular cylinder more than that on a square section. In the lock-in regime a square section is only unstable to vortex shedding at the high-reduced-velocity end. These fundamental differences in flow behaviour will need to be taken into account in the adaptation of mathematical models to predict square-cylinder response to vortex shedding. In addition, as discussed by Wawzonek & Parkinson (1979), if the critical reduced velocity for the onset of galloping, as predicted by quasisteady theory, is at or below vortex lock-in we can expect a complex merging, at the upper end of lock-in, of the response due to vortex shedding with that due to galloping.

The flow around a square-section cylinder was visualized using smoke, and figure 20 (*a*) shows a photograph of the wake for an amplitude ratio of 0·25 and a reduced velocity in the middle of the lock-in range. The flow pattern is little different from that observed behind a fixed square section, but in the oscillating case the vortices are more clearly defined. The photograph in figure 20 (*b*), taken at the same amplitude ratio but at a reduced velocity of 4, shows a completely different wake structure. The shear

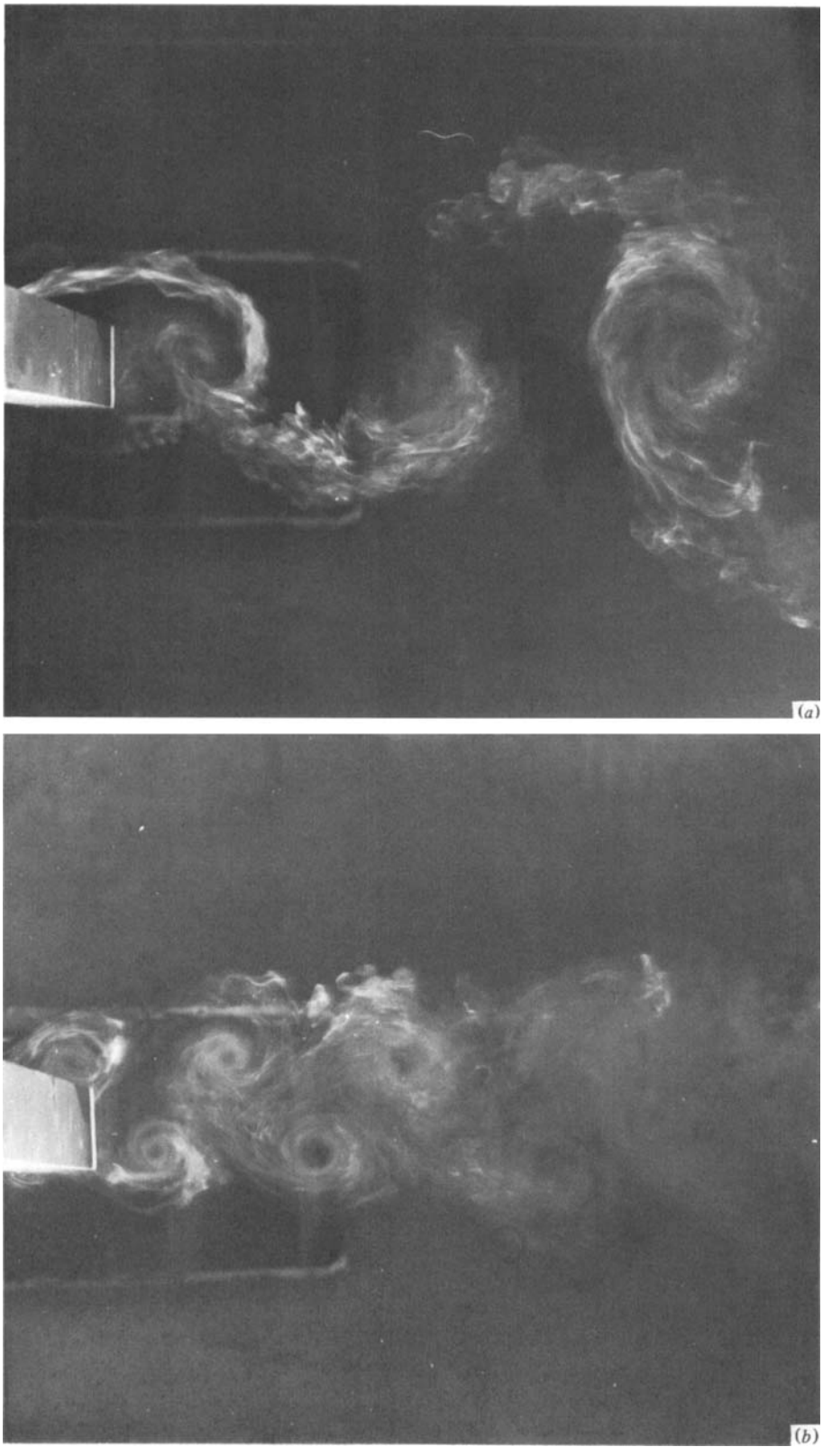

FIGURE 20. Visualization of the flow around an oscillating square-section cylinder. (*a*) $A/D = 0{\cdot}25$, $U/ND = 7{\cdot}8$; (*b*) 0·25, 4·0.

layers separating from the upstream corners roll up to form vortices over the side faces of the body, creating high suctions there, and are discharged into the wake at the oscillation frequency. During part of the cycle there appears to be a reattachment of the flow to the side faces. Expressed as a Strouhal number, the non-dimensional frequency of these vortices is substantially higher than that for a stationary square-section cylinder, and is equal simply to the inverse of the reduced velocity.

Comparing figures 20(*a*) and (*b*), it is clear that the spacing of vortices in the wake and the vortex-formation process are different. The mechanism for vortex formation (as proposed by Gerrard (1966) and visualized in figure 20(*a*)) of two shear layers separating and interacting, to develop discrete vortices by mutual induction across the near wake, is not observed behind a square-section cylinder oscillating at low values of reduced velocity. Further evidence that a dramatic change occurs in the flow at low values of reduced velocity is provided by the values of time-mean base pressure shown in figure 4, where it can be seen that the pressure coefficient in the centre of the base changes from $-1{\cdot}6$ when the body is stationary to $-0{\cdot}54$ when it is oscillating at a reduced velocity of about 4 and at an amplitude equal to only 10 % of D. Hence, whereas above lock-in the effects of transverse body oscillation can be accounted for by a quasisteady analysis, below lock-in a strong interaction takes place between the flow and body movement.

5. Conclusions

Mean and fluctuating pressures were measured on a square-section cylinder, with one face normal to the upstream flow, forced to oscillate with amplitude ratios up to 0·25 and reduced velocities in the range 4–13. Vortex lock-in was observed in the neighbourhood of the resonant velocity, and the extent of the lock-in range increased with increasing oscillation amplitude. Fluctuating-surface-pressure measurements showed that the flow was almost fully correlated across the span of the model at lock-in. On the side faces the coefficient of fluctuating pressure increased in the lock-in regime above its value for the stationary model. The sectional coefficient of fluctuating lift was calculated from measurements of fluctuating surface pressure, and at lock-in and an amplitude ratio of 0·25 it was found that the coefficient was about 54 % greater than that found for the stationary model. Traces of surface-pressure signals indicate that, in the lock-in range, body oscillation reduces the amount of amplitude modulation but it does not significantly increase peak values. Measurements of fluctuating lift showed trends with increasing amplitude similar to those measured by Nakamura & Mizota (1975) and Otsuki *et al.* (1974), although magnitudes are not in close agreement.

Substantial differences are noted between the flow around an oscillating square-section and that around an oscillating circular cylinder. The circular cylinder showed a much greater amplification of fluctuating surface pressures in the lock-in regime. The phase of the lift relative to the cylinder displacement is positive throughout the lock-in range for a circular cylinder, whereas for a square section it is only positive towards the upper end of the lock-in range. Hence spring-mounted, square-section cylinders will only oscillate as a result of vortex shedding at reduced velocities above the resonant value. These observed features of the flow around an oscillating square

section will need to be accounted for in any application to this shape of mathematical models developed to predict circular cylinder response.

Body oscillation is found to modify the flow substantially at reduced velocities below lock-in. Vortices form over the side faces and shed into the wake at the body frequency. During a shedding cycle reattachment occurs on the side faces, and the base pressure is increased substantially. It is estimated that at a reduced velocity of four and an amplitude ratio of 0·1 the mean drag is more than 40 % less than its value for a stationary cylinder. At these low values of reduced velocity the phase of the shedding is such as to damp out oscillations of a flexibly mounted cylinder.

The authors would like to thank the workshop staff for constructing the models and the forced oscillation rig used in this investigation. The design of the oscillation apparatus is due to P. Gasson and M. E. Davies. One of the authors (E. D. O.) was supported by the Commonwealth Scholarship Commission.

REFERENCES

BEARMAN, P. W. & CURRIE, I. G. 1979 Pressure-fluctuation measurements on an oscillating circular cylinder. *J. Fluid Mech.* **91**, 661–677.

BEARMAN, P. W. & GRAHAM, J. M. R. 1979 Hydrodynamic forces on cylindrical bodies in oscillatory flow. In *Proc. 2nd Int. Conf. on the Behaviour of Offshore Structures, London*, pp. 309–322.

BEARMAN, P. W. & TRUEMAN, D. M. 1971 An investigation of the flow around rectangular cylinders. *I.C. Aero. Rep.* no. 71–15.

BERGER, E. & WILLE, R. 1972 Periodic flow phenomena. *Ann. Rev. Fluid Mech.* **4**, 313–340.

BISHOP, R. E. D. & HASSAN, A. Y. 1964*a* The lift and drag forces on a circular cylinder in a flowing fluid. *Proc. R. Soc. Lond.* A **277**, 32–50.

BISHOP, R. E. D. & HASSAN, A. Y. 1964*b* The lift and drag forces on a circular cylinder oscillating in a flowing fluid. *Proc. R. Soc. Lond.* A **277**, 51–75.

DAVIES, M. E. 1975 Wakes of oscillating bluff bodies. Ph.D. thesis, Department of Aeronautics, Imperial College, London.

DAVIES, M. E. 1976 A comparison of the wake structure of a stationary and oscillating bluff body, using a conditional averaging technique. *J. Fluid Mech.* **75**, 209–231.

GERRARD, J. H. 1966 The mechanics of the formation region of vortices behind bluff bodies. *J. Fluid Mech.* **25**, 401–413.

HARTLEN, R. T. & CURRIE, I. G. 1970 Lift-oscillator model of vortex-induced vibrations. *Proc. A.S.C.E.* **96** (EMD), 577–591.

LEE, B. E. 1975 The effect of turbulence on the surface pressure field of a square prism. *J. Fluid Mech.* **69**, 263–282.

MASKELL, E. C. 1963 A theory of blockage effects on bluff bodies and stalled wings in a closed wind tunnel. *A.R.C., R. & M.* no. 3400.

NAKAMURA, Y. & MIZOTA, T. 1975 Unsteady lifts and wakes of oscillating rectangular prisms. *Proc. A.S.C.E.* **101** (EM6), 855–871.

OBASAJU, E. D. 1979 On the effects of end plates on the mean forces on square sectional cylinders. *J. Ind. Aero.* **5**, 179–186.

OTSUKI, Y., WASHIZU, K., TOMIZAWA, H. & OHYA, A. 1974 A note on the aeroelastic instability of a prismatic bar with square sections. *J. Sound Vib.* **34**, 233–248.

PARKINSON, G. V. 1974 Mathematical models of flow-induced vibrations. In *Flow-Induced Structural Vibrations* (ed. E. Naudascher). Springer.

POCHA, J. J. 1971 On unsteady flow past cylinders of square cross-section. Ph.D. thesis, Department of Aeronautics, Queen Mary College, London.

ROSHKO, A. 1954 On the drag and shedding frequency of two-dimensional bluff bodies. *NACA TN* no. 3169.

SARPKAYA, T. 1978 Fluid forces on oscillating cylinders. *Proc. A.S.C.E.* (WW4) 275–290.

SARPKAYA, T. 1979 Vortex-induced oscillations. *Trans. A.S.M.E.* E, *J. Appl. Mech.* **46**, 241–258.

STANSBY, P. K. 1976 Base pressure of oscillating circular cylinders. *Proc. A.S.C.E.* **102** (EM4), 591–600.

TANIDA, Y., OKAJIMA, A. & WATANABE, Y. 1973 Stability of a circular cylinder oscillating in uniform flow or in a wake. *J. Fluid Mech.* **61**, 769–784.

VICKERY, B. J. 1966 Fluctuating lift and drag on a long cylinder of square cross-section in a smooth and in a turbulent stream. *J. Fluid Mech.* **25**, 481–494.

WAWZONEK, M. A. & PARKINSON, G. V. 1979 Combined effects of galloping instability and vortex resonance. In *Proc. 4th Int. Conf. on Wind Effects on Buildings and Structures, Fort Collins, Colorado.*

WILKINSON, R. H. 1974 On the vortex-induced loading on long bluff cylinders. Ph.D. thesis, Faculty of Engineering, University of Bristol, England.